Study of the nonequilibrium critical quenching and the annealing dynamics for the long-range Ising model in one dimension

J. Stat. Mech. (2011) P09007

(http://iopscience.iop.org/1742-5468/2011/09/P09007)

Journal of Statistical Mechanics: Theory and Experiment
An IOP and SISSA journal

Study of the nonequilibrium critical quenching and the annealing dynamics for the long-range Ising model in one dimension

D E Rodriguez[1], M A Bab[2] and E V Albano[3]

[1] Instituto de Física de Líquidos y Sistemas Biológicos (IFLYSIB), calle 59 nro 789 (1900), Universidad Nacional de La Plata, CCT-La Plata CONICET, La Plata, Argentina
[2] Instituto de Investigaciones Fisicoquímicas Teóricas y Aplicadas (INIFTA), Facultad de Ciencias Exactas, Universidad Nacional de La Plata, CCT-La Plata CONICET, Sucursal 4, CC16 (1900) La Plata, Argentina
[3] Instituto de Física de Líquidos y Sistemas Biológicos, Facultad de Ciencias Exactas, Universidad Nacional de La Plata, CCT-La Plata CONICET, La Plata, Argentina
E-mail: rodrigdiego@gmail.com, mbab@inifta.unlp.edu.ar and ezequielalb@yahoo.com.ar

Received 14 April 2011
Accepted 12 August 2011
Published 14 September 2011

Online at stacks.iop.org/JSTAT/2011/P09007
doi:10.1088/1742-5468/2011/09/P09007

Abstract. Extensive Monte Carlo simulations are employed in order to study the dynamic critical behaviour of the one-dimensional Ising magnet, with algebraically decaying long-range interactions of the form $1/r^{d+\sigma}$, with $\sigma = 0.75$. The critical temperature, as well as the critical exponents, are evaluated from the power-law behaviour of suitable physical observables when the system is quenched from uncorrelated states, corresponding to infinite temperature, to the critical point. These results are compared with those obtained from the dynamic evolution of the system when it is annealed at the critical point from the ordered state. Also, the critical temperature in the infinite interaction limit is obtained by means of a finite-range scaling analysis of data measured with different truncated interaction ranges. All the estimated static critical exponents (γ/ν, β/ν, and $1/\nu$) are in good agreement with renormalization group (RG) results and previously reported numerical data obtained under equilibrium conditions. On the other hand, the dynamic exponent of the initial increase of the magnetization (θ) was

1742-5468/11/P09007+17$33.00

close to RG predictions. However, the dynamic exponent z of the time correlation length is slightly different to the RG results probably due to the fact that it may depend on the specific dynamics used or because the two-loop expansion used in the RG analysis may be insufficient.

Keywords: classical Monte Carlo simulations, classical phase transitions (theory), critical exponents and amplitudes (theory), finite-size scaling

Contents

1. Introduction

The study of the critical behaviour of systems with long-range (LR) interactions is still a challenging topic in the field of statistical physics [1]–[4]. Furthermore, the understanding of the dynamic evolution of these systems, from far-from-equilibrium initial states towards a final equilibrium regime, poses an additional difficulty due to the fast relaxation of relevant physical observables owing to the presence of LR interactions. For these reasons, the study of relaxation processes in simple Ising and Potts models with LR interactions plays an important role for the understanding of the dynamics of second-order phase transitions. Within this context, the study of the short-time dynamics (STD) of critical systems has attracted great attention during the last two decades [1], [5]–[7]; for a recent review see [8]. The pioneering theoretical study of the STD, which was formulated in the context of the dynamic renormalization group [9], predicts the existence of a new exponent related to the initial increase of the order parameter. This prediction has subsequently been validated by a large body of numerical evidence obtained in a variety of models [5, 8], [10]–[14]. However, only few studies have been performed in order to generalize these concepts to systems with LR interactions. In fact, the field-theoretical calculations of Janssen *et al* [9] have been extended to the case of LR interactions decaying according to a power law for the case of the continuous n-vector model [1], the random Ising model [15],

J. Stat. Mech. (2011) P09007

and the kinetic spherical model [16, 17], and only a few preliminary numerical results on the STD of the LR Potts model have been reported [7]. On the other hand, theoretical studies of the relaxation dynamics of discrete models are still lacking. Recently, numerical results on the relaxation dynamics of the LR Ising model, obtained by applying a new algorithm that produces effective long-range interactions, have been reported [18].

In order to contribute to the understanding of the dynamics of phase transitions in discrete systems, our aim in this paper is to report and discuss extensive numerical simulations of the Ising model, in one dimension, with LR interactions decaying with the distance as a power law. For this purpose, we performed studies of both the STD of initially disordered states (i.e., quenching experiments) and the relaxation dynamics of initially ordered states (i.e., annealing experiments). Since the term annealing has a wide range of interpretations, in order to avoid misunderstandings in this paper we refer to the case where the system at the initial temperature ($T = 0$) is suddenly heated up to a pre-established T that remains constant. Results obtained by applying these methods allow us to determine not only the critical temperature, but also the complete set of static and dynamic critical exponents (for the methodology used, see e.g. [8, 19]). In this way, we can compare our results with theoretical renormalization group (RG) results [1, 20], with independent numerical determinations of the static exponents performed under equilibrium conditions [2], and with the results reported in [7, 18].

The paper is organized as follows: in section 2 a brief description of the model and the simulation method is presented, section 3 is devoted to a brief discussion of the theoretical background subsequently applied to the analysis of the results that are discussed in section 4, and finally, our conclusions are stated in section 5.

2. The Ising model with LR interactions and the simulation method

In this paper we present and discuss simulations of the LR Ising model in $d = 1$ dimension, whose Hamiltonian, H, is given by

$$H = -J \sum_{\langle i,j \rangle} S_i S_j / r_{ij}^{d+\sigma}, \tag{1}$$

where $J > 0$ is the (ferromagnetic) coupling constant, S_i is the spin variable at the site of coordinates i, which can assume two values, $S_i = \pm 1$, the summation is extended to all pairs of spins placed at distances $r_{i,j} = |r_i - r_j|$, and σ is a parameter that controls the decay of LR interactions.

Simulations are performed by using samples of length $L \leq 1 \times 10^5$ and taking periodic boundary conditions. The LR interactions described by the Hamiltonian of equation (1) are evaluated up to a distance $|r_i - r_j| = L/2$. Also, simulations with LR interactions truncated at the Nth neighbour, i.e., $J = 0$ for $r > N$, have been performed in order to apply a finite-range scaling (FRS) analysis [21], and the results will be briefly discussed. Spin update is performed by using the standard Metropolis dynamics. Also, during a Monte Carlo time step (MCS) all the spins of the sample are updated once, on average.

In order to carry out the calculations we chose $\sigma = 0.75$, because for this value of the parameter the critical exponents of the Ising model are expected to be sufficiently different from mean-field values ($\sigma = 0.50$) to allow a meaningful comparison with RG

J. Stat. Mech. (2011) P09007

results [22]–[24]. Furthermore, one also likes to be as far as possible from $\sigma = 1.00$, where strong Kosterlitz–Thouless behaviour is known to occur [25].

During the simulations we recorded the time dependence of the following observables: (i) the order parameter or average magnetization ($M(t,\tau)$) given by

$$M(t,\tau) = \frac{1}{L}\left\langle \sum_{i=1}^{L} S_i(t,\tau) \right\rangle, \tag{2}$$

where $\tau = (T - T_c)/T_c$ is the reduced temperature and T_c is the critical temperature.

(ii) The susceptibility ($\chi(t,\tau)$) evaluated as the fluctuations of the order parameter, namely

$$\chi(t,\tau) = (M^2(t,\tau) - M(t,\tau)^2), \tag{3}$$

where $M^2(t,\tau) = 1/L^2\langle(\sum_{i=1}^{L} S_i(t,\tau))^2\rangle$.

(iii) The autocorrelation of the spin variable

$$A(t,\tau) = \frac{1}{L}\left\langle \sum_{i=1}^{L} S_i(t,\tau)S_i(0,\tau) \right\rangle. \tag{4}$$

(iv) The time correlation of two spins separated by a distance r at the critical point

$$C(t,r) = \frac{1}{L}\left\langle \sum_{i=1}^{L} S_i(t)S_{i+r}(t) \right\rangle. \tag{5}$$

(v) The autocorrelation of the order parameter at the critical point, when the initial condition corresponds to uncorrelated states, given by

$$Q(t) = \frac{1}{L^2}\left\langle \sum_{i=1}^{L} S_i(t) \sum_{i=1}^{L} S_i(0) \right\rangle. \tag{6}$$

(vi) The second-order Binder cumulant ($U(t)$), when the initial condition corresponds to the ground state, namely,

$$U(t,\tau) = \frac{M^2(t,\tau)}{M(t,\tau)^2} - 1, \tag{7}$$

where in all cases the brackets indicate configurational averages performed over a number n_s of different samples starting from equivalent (but different in the case of $T = \infty$) initial conditions.

3. A brief theoretical background

Short-time dynamics (STD). Let us now analyse the expected short-time dynamic behaviour when the system starts from a disordered (uncorrelated) configuration, but with a small initial magnetization. According to the argument of Janssen *et al* [9], the general scaling approach for the order parameter for the nonconservative dynamics of model A (according to the classification of Hohenberg and Halperin [26]) is given by

$$M(t,\tau,L,M_0) = b^{-\beta/\nu} M\ (t/b^z, b^{1/\nu}\tau, L/b, b^{x_0}M_0), \tag{8}$$

J. Stat. Mech. (2011) P09007

where b is a scaling parameter, and β and ν are the order parameter and correlation length (static) critical exponents, respectively. Also, z is the dynamic exponent. Furthermore, x_0 is a new exponent, introduced by Janssen *et al* [9], which accounts for the scaling dimension of the initial magnetization M_0, in the $M_0 \to 0$ limit.

For sufficiently large lattices, at the critical point ($\tau \equiv 0$), and on setting $b = t^{1/z}$, equation (8) becomes

$$M(t, M_0) = t^{-\beta/\nu z} M(t^{x_0/z} M_0), \tag{9}$$

which holds for a time short enough that the correlation length ($\xi(t) \propto t^{1/z}$) is not so large ($\xi \ll L$). Furthermore, for times even shorter than the crossover time ($t_x \approx M_0^{-z/x_0}$), but larger than the microscopic time ($t_{\rm mic}$) that is set when the correlation length is of the order of a single lattice spacing, equation (9) becomes

$$M(t) \propto M_0 t^{\theta}, \tag{10}$$

which describes the (power-law) initial increase of the magnetization with exponent $\theta = x_0/z - \beta/\nu z$.

In the absence of an initial magnetization ($M_0 \equiv 0$), and at criticality, the scaling behaviour of the susceptibility is given by

$$\chi(t) \propto t^{\gamma/\nu z}, \tag{11}$$

where γ is the susceptibility exponent. Also, under these conditions ($\tau = 0$ and $M_0 = 0$), the time autocorrelation function is expected to follow a power law with time according to

$$A(t) \propto t^{-\lambda}, \tag{12}$$

where the critical exponent is given by $\lambda = d/z - \theta$, i.e., even in the absence of an initial magnetization, λ depends on the exponent θ that describes the initial increase of the order parameter according to equation (10).

On the other hand, on starting with randomly generated configurations, the correlation function of the magnetization is also expected to follow a power law with time according to

$$Q(t) \propto t^{\theta}, \tag{13}$$

i.e., a relationship that allows us to obtain the initial increase exponent avoiding the numerical extrapolation $M_0 \to 0$ [6].

Finally, the two-spin time correlation allows us to obtain an independent determination of dynamic exponent z by means of the following scaling form [27]

$$C(t, r) = r^{-(d-2+\eta)} C(r/\xi(t)). \tag{14}$$

Standard relaxation dynamics (SRD). STD measurements can be further reinforced by independent measurements of the SRD, which are started from a fully ordered or ground state configuration and are performed at criticality. In this way, one could be able not only to test the validity of some exponents evaluated by means of the STD method, as well as the critical temperature, but also to obtain additional exponents and test the validity of relationships between them, e.g., the hyperscaling relationship [5]. In fact, by starting from a ground state configuration with all spins pointing in the same direction ($T = 0$)

J. Stat. Mech. (2011) P09007

and annealing the system at criticality, the SRD scaling approach is given by (see also equation (9))

$$M(t,\tau,L) = b^{-\beta/\nu} M(t/b^z, b^{1/\nu}\tau, L/b). \tag{15}$$

For large lattices and on setting $b = t^{1/z}$, this dynamic scaling form leads to

$$M(t,\tau) \propto t^{-\beta/\nu z} M(t^{1/\nu z}\tau). \tag{16}$$

It is well known that this power-law decay of the order parameter is valid within the long-time regime, but several numerical results indicate that it also holds in the short-time regime.

On the other hand, by taking the logarithmic derivative of equation (16) with respect to the reduced temperature, evaluated at the critical point, one gets

$$\left.\frac{\partial \log M(t,\tau)}{\partial \tau}\right|_{\tau=0} \propto t^{1/\nu z}, \tag{17}$$

which allows us to evaluate the exponent $1/\nu z$ by performing measurements at and slightly away from the critical point. Furthermore, just at the critical point the second-order Binder cumulant is expected to behave according to

$$U(t) \propto t^{d/z}. \tag{18}$$

It is worth mentioning that because of the small nonequilibrium correlation length for short-ranged models, both STD and SRD are free of finite-size effects. However, in long-ranged models, finite-size effects also appear due to the fact that the finite size yields a truncated interaction range. So, this effect remains even during the short-time regime investigated in this paper and it is worth knowing its influence on both the critical temperature and the critical exponents.

4. Results and discussion

4.1. Standard relaxation dynamics

Focusing our attention first on the relaxation dynamic behaviour at criticality, figure 1 shows the time evolution of the magnetization at different temperatures for the system size $L = 2 \times 10^4$. It is well known that for temperatures close to the critical point, deviations from the expected power-law behaviour given by equation (16) are due to at least three different contributions. (i) As follows from the scaling function involved in equation (16) one has a downward (upward) deviation for $T > T_c$ ($T < T_c$). (ii) Also, close to criticality, finite-size effects and (iii) the finite range of the interactions considered are identified by means of a drop in the time evolution of the order parameter, which takes place at a time around $t_{end}(L)$ that depends on the system size. Therefore, all effects cause deviations, hindering the determination of t_{end}. So, let us briefly describe here the method used throughout the paper in order to determine the critical points and the critical exponents, as well the corresponding error bars. We notice that by means of a simultaneous analysis of the behaviour of $\mathrm{d}(\log(M))/\mathrm{d}(\log(t))$ and the observation of the best power-law behaviour obtained for the largest system size, we can overcome these shortcomings and obtain a reliable estimate of $t_{end}(L)$. In fact, as shown in the inset of figure 1, upward (downward) departures form the power law correspond to $T < T_c$

J. Stat. Mech. (2011) P09007

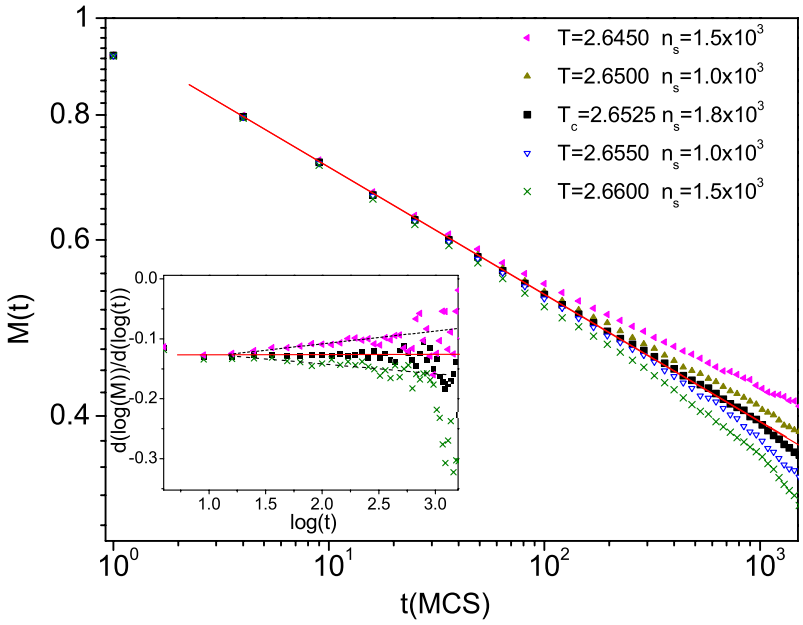

Figure 1. Log–log plots of the time evolution of the magnetization $M(t)$ obtained on annealing from $T = 0$ (ground state) at the indicated temperatures. The data correspond to the system size $L = 2\times10^4$. The solid line shows the fit of the curve obtained for $T_c = 2.6525$, according to equation (16). The number of averaged configurations (n_s) is also indicated. The inset shows the derivative of $\log(M)$ with respect of $\log(t)$; the solid line corresponds to $\beta/\nu z = 0.129$. More details appear in the text.

($T > T_c$), while the critical temperature corresponds to a constant value within of the time interval (t_{mic}, t_{end}), which gives the value of the critical exponent involved. On the other hand, deviations from the horizontal behaviour in the curve corresponding to T_c (see the inset of figure 1) are due to the operation of both finite-size and finite-range effects, a fact that allows us to estimate $t_{end}(L)$. Then, for the system size $L = 2 \times 10^4$ shown in figure 1, the critical temperature $T_c = 2.6525(25)$ was found. The error bars of T_c were assessed by considering the closest temperatures that present noticeable but small deviations from the power-law behaviour. Also, from the fit of the data the critical exponent $\beta/\nu z = 0.129(6)$ was determined (see also the horizontal line in the inset of figure 1).

4.1.1. Finite-size effects. In order to investigate the influence of finite-size effects on the results, the procedure described above was carried out not only for several system sizes (see figure 2), but also for different interaction ranges. The purpose of that type of study is to distinguish between two different sources of size effects: those caused by the finiteness of the sample and others caused by the finite interaction range. In fact, in contrast to the case of results often obtained by using models with short-range interactions [8], here the expected power-law behaviour of the physical observables is observed for temperatures that depend on the size, i.e. effective critical temperatures. Then it is possible to understand this situation as an additional size effect that is caused

J. Stat. Mech. (2011) P09007

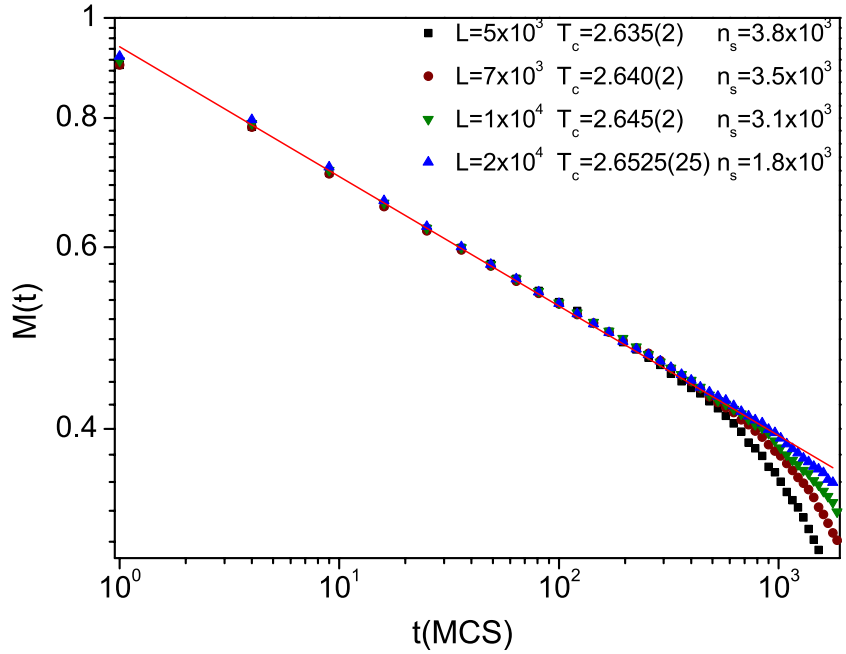

Figure 2. Log–log plot of the time evolution of the magnetization $M(t)$ obtained on annealing from $T = 0$ (ground state) to the critical temperatures corresponding to the indicated system sizes (L). The solid line shows the fit of the curve obtained for $L = 10^4$. The number of averaged configurations (n_s) is also indicated. More details appear in the text.

by the truncated interaction range of the long-range interaction rather than by the usual finite number of spin sites considered in Monte Carlo simulations. Indeed, a finite-system-size sample implies a truncated interaction range, i.e., the maxima number of neighbours ($N_{\max}$) on either side of the central spin considered in order to evaluate the Hamiltonian given by equation (1) is finite, and due to the periodic boundary conditions used, one has $N_{\max} = L/2$. Following that, simulations with different $N \leq N_{\max}$ and L values were carried out. Figure 3 shows the critical relaxation of the magnetization for a system size $L = 10^4$ and different N values. The data indicate that the effective critical temperature and the range of the power-law behaviour depend on the value of N but the corresponding critical exponent remains unaffected, within the short-time regime. Furthermore, this statement is reinforced by the results shown in figures 4(a) and (b) that correspond to $N = 2 \times 10^3$ and $N = 5 \times 10^3$, and different L values, respectively.

Summing up, the (almost) perfect overlap of the curves observed within the suitable time interval defined for each system size shows that in the LR Ising model the critical temperature must be changed with the size, while the critical exponents are no longer influenced.

4.1.2. Finite-range scaling (FRS) analysis. A FRS analysis has also been applied in order to obtain the critical temperature in the infinite interaction range (thermodynamic limit). This type of analysis has already been developed by analogy with the finite-size scaling method [21]. The basic idea behind this approach is to study systems with different

J. Stat. Mech. (2011) P09007

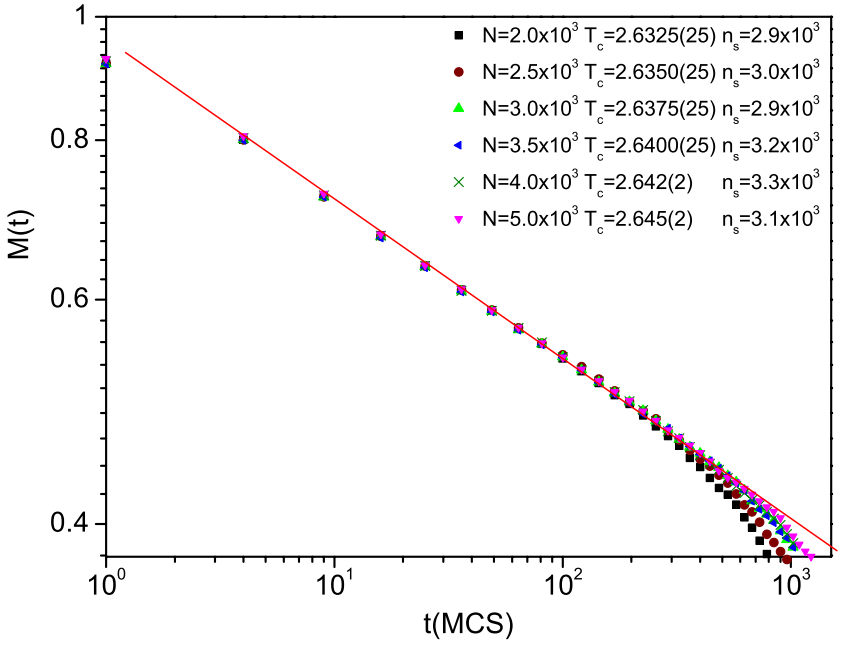

Figure 3. Log–log plot of the critical relaxation of the magnetization $M(t)$ from $T = 0$ for the system size $L = 10^4$ and different interaction ranges N. The solid line shows the fit of the curve obtained for $N = 5 \times 10^3$. The numbers of averaged configurations (n_s) and effective critical temperatures are also indicated. More details appear in the text.

truncated interaction ranges and obtain information on the critical behaviour by means of scaling properties. In this way, on the basis of [21], the following scaling dependence has been proposed:

$$T_c(N) = T_c(\infty) + A/N^{x_T}, \tag{19}$$

where $T_c(\infty)$ is the critical temperature for the infinite interaction range, x_T is the convergence exponent, and A is a constant. According to standard finite-size scaling we assume that $x_T = 1/\nu$ [28, 29]. Figure 5 shows the $T_c(N)$ values obtained as a function of $N^{-1/\nu}$, which was fitted with the aid of equation (19) (continuous line) and gives the critical temperature ($T_c(\infty) = 2.669(1)$). The critical temperature obtained by this approach interpolates between the previously reported values for $\sigma = 0.70$ ($T_c(\infty) = 2.929$ [21] and $T_c(\infty) = 2.9269$ [31]), and for $\sigma = 0.80$ ($T_c(\infty) = 2.431$ [21] and $T_c(\infty) = 2.4299$ [31]), which were obtained by means of analytic calculations with the transfer matrix method and FRS analysis.

Also, in figure 5 we have included the value reported by Tomita [18] (after a proper interpolation) for $N = 2^{22}$, which within the error bars is in full agreement with our results. This fact also shows that the algorithm used in [18] gives (non-universal) effective critical temperatures that are in agreement with the standard Metropolis algorithm.

4.1.3. Critical exponents. The already discussed results suggest that the system size $L = 10^4$ is large enough for the evaluation of the critical exponents within a suitable

J. Stat. Mech. (2011) P09007

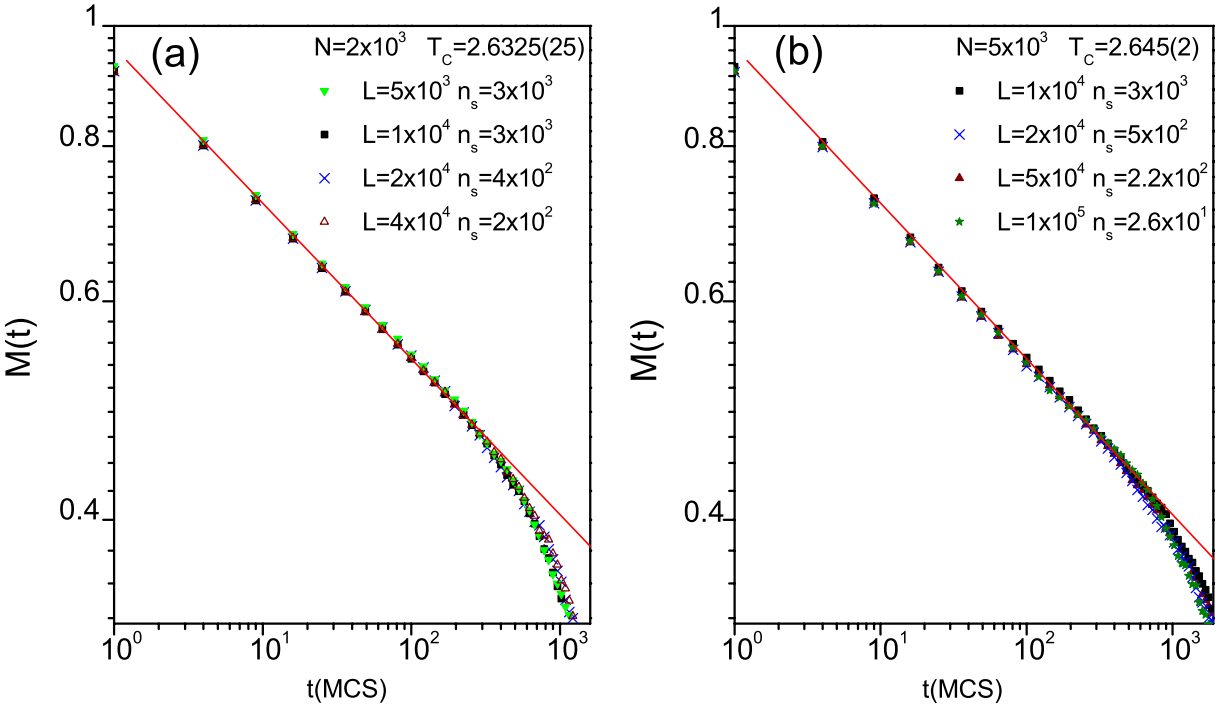

Figure 4. Log–log plot of the critical relaxation of the magnetization $M(t)$ from $T = 0$ for the system sizes L indicated and fixed interaction range: (a) $N = 2\times10^3$ and (b) $N = 5\times10^3$. The solid lines correspond to the fits, which give an exponent $\beta/\nu z = 0.129(6)$. The numbers of averaged configurations (n_s) and effective critical temperatures are also indicated. More details appear in the text.

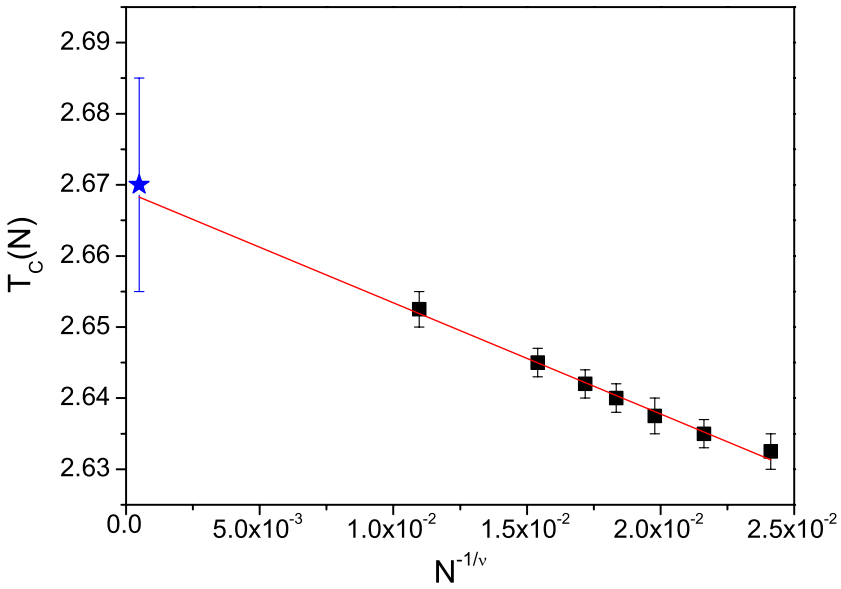

Figure 5. Plot of the effective critical temperature as a function of $N^{-1/\nu}$ (full squares). The continuous line corresponds to the fit performed with the aid of equation (19). The effective critical temperature reported in [18] is also included (full star). More details appear in the text.

J. Stat. Mech. (2011) P09007

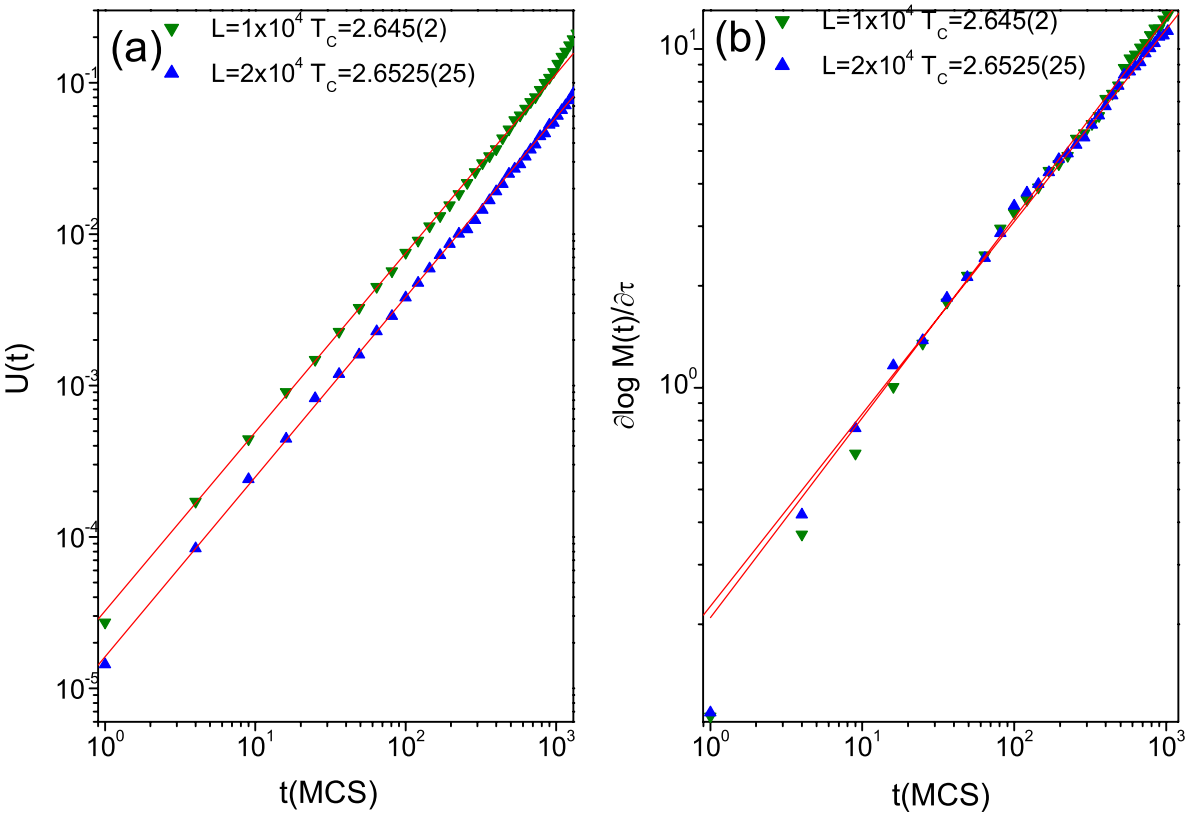

Figure 6. Time evolutions of dynamic observables obtained on annealing at the effective critical temperature from $T = 0$. (a) The second-order Binder cumulant ($U(t)$), and (b) the logarithmic derivative of the magnetization with respect to the reduced temperature ($\partial \log(t)/\partial\tau$). The solid lines indicate the fits performed with the aid of equations (17) and (18), respectively. The system sizes (L) and the corresponding effective critical temperatures (T_c) are also indicated.

time interval, namely (10, 900) MCS. In order to verify the above statement and to obtain the complete set of critical exponents, the SRD of the physical observables was obtained for system sizes of $L = 10^4$ and 2×10^4 up to 10^3 MCS. Figure 6(a) shows the time evolution of the second-order Binder cumulant at the effective critical temperature that can be fitted with a power law with the exponents listed in table 1 (third column). From these values the dynamic exponent z was estimated to be close to $z = 0.84(2)$ (see table 1, fifth column), i.e. a figure that is significantly larger than the RG results, given by $z_{\mathrm{RG}} = 0.775$ [1]. In principle one could expect this disagreement to be most likely due to the fact that z depends on the specific dynamics used, as in the case of the short-ranged Ising model [32]. Nevertheless, this discrepancy could also be attributed to an underestimation of the RG calculation, again as in the case of the short-ranged Ising model [33]. Furthermore, the dynamic exponent obtained interpolates between the values reported by Tomita [18], i.e. $z = 0.79(4)$ and $1.00(1)$ for $\sigma = 0.70$ and 0.80, respectively.

On the other hand, by using measurements of the magnetization performed at two temperature points adjacent to the effective critical one, the logarithmic derivative of the magnetization with respect to the reduced temperature was obtained. Figure 6(b) shows

J. Stat. Mech. (2011) P09007

Table 1. List of exponents obtained by means of SRD measurements of the magnetization ($\beta/\nu z$), Binder cumulant (d/z), and logarithmic derivative of the magnetization with respect to the reduced temperature ($1/\nu z$). The estimated critical exponents z, $1/\nu$, and β/ν, as well as the RG predictions, are also listed for the sake of comparison.

L	$\beta/\nu z$	d/z	$1/\nu z$	z	$1/\nu$	β/ν
1×10^4	0.129(7)	1.20(2)	0.59(2)	0.83(1)	0.49(2)	0.107(5)
2×10^4	0.129(6)	1.19(3)	0.57(2)	0.84(2)	0.48(2)	0.109(6)
RG				0.775	0.4765	0.125

that this observable also exhibits a power-law behaviour and the fitted exponents are listed in table 1, fourth column. Furthermore, by replacing the value obtained for z in the exponent corresponding to the logarithmic derivative, one gets $1/\nu = 0.48(2)$ (see table 1, sixth column), in agreement with both the RG prediction, namely, $1/\nu = 0.4765$ [1, 20], and the Monte Carlo simulations performed at equilibrium, $1/\nu = 0.469$ [20]. Finally, from the exponents β/ν and $1/\nu$ one can obtain the SRD estimation of $\beta/\nu = 0.109(6)$ that also interpolates between the values reported in [18].

It is worth mentioning that the error bars of the evaluated exponents are not easy to estimate because they are introduced by several sources such as insufficient statistics, arbitrariness in the time interval used to fit the power-law behaviour of the observables, and, finally, the use of an approximate effective critical temperature, T_c. In order to have an estimation of the magnitude of the error due to the former source, a variant of the blocking method was used [30]. For this purpose one proceeds as follows: the time dependence of each observable is fitted for several independent sets of measurements; then, the error bars are obtained by accounting for the spreading of the obtained values. In the case of the time interval used for the power-law fit, we found that the selection of the microscopic time $t_{\rm mic}$ accounts for the major error. So, the reported exponents correspond to a fixed $t_{\rm mic}$ that is established after the first 10 MCS, and the error bars include the values obtained by taking $t_{\rm mic}$ within the range 10–100 MCS. On the other hand, the error due to the approximate critical temperature cannot be estimated directly.

4.2. Short-time dynamics

Now we turn our attention to the STD measurements. The STD evolution exhibits a weak dependence on the quenching temperature, so this shortcoming hinders an independent estimation of T_c. Consequently, in the simulations we used the values obtained from SRD measurements. As in that case, a finite-size analysis of the time evolution of the susceptibility (see figure 7(a)) allows us to determine the suitable time interval to be used in order to perform the fitting procedure. In this way, for the system size $L = 10^4$ the power-law behaviour is observed up to 400 MCS. Also, the autocorrelation function (figure 7(b)) exhibits a power-law decay at the same time interval. The critical exponents $\gamma/\nu z$ and λ obtained by means of fits with the aid of equations (11) and (12), respectively, are presented in table 2. The error bars of the critical exponents were estimated in the same way as for the case of the SRD measurements, and they include the values corresponding to $t_{\rm mic}$ taken from the interval 4–36 MCS.

J. Stat. Mech. (2011) P09007

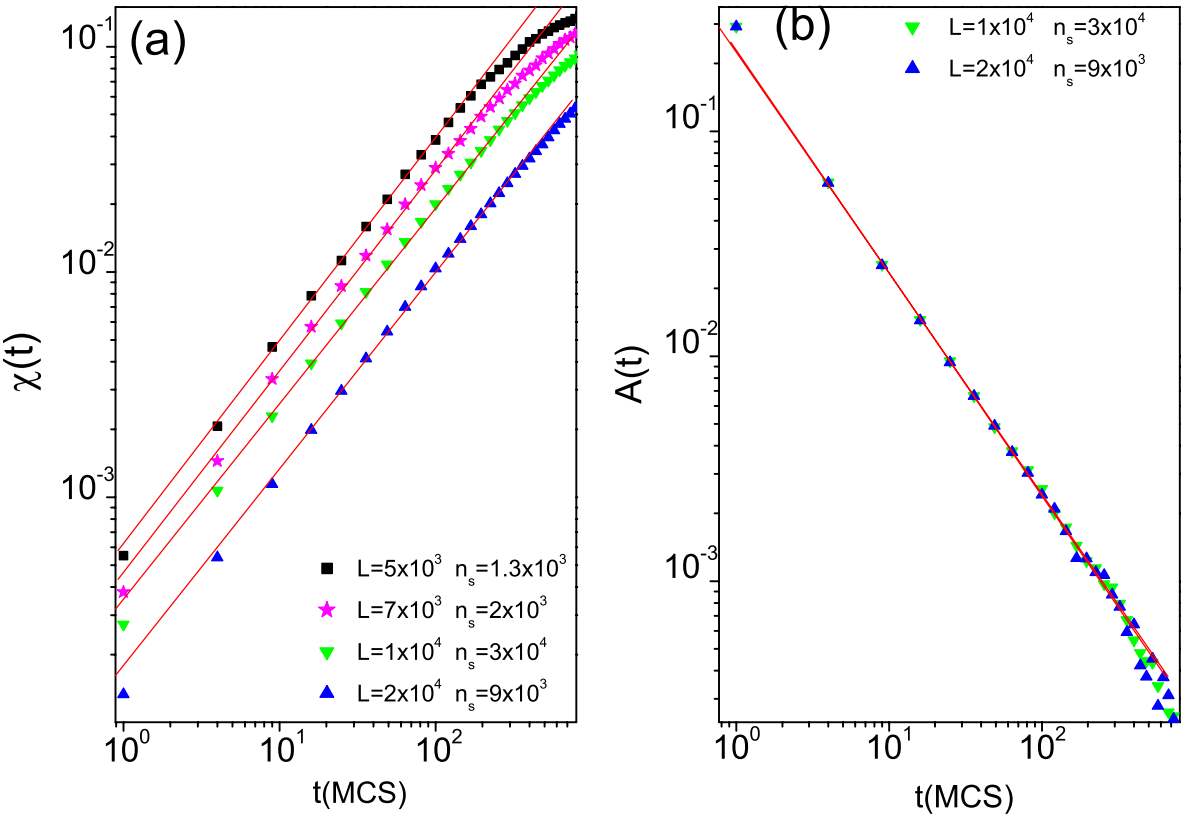

Figure 7. Time evolution measured after quenching from uncorrelated (disordered) states to the corresponding effective critical temperature T_c of (a) the susceptibility $\chi(t)$ and (b) the autocorrelation $A(t)$. The solid lines indicate the fits performed with the aid of equations (11) and (12), respectively. The number of averaged configurations (n_s) and the system sizes (L) are also indicated.

Table 2. Critical exponents obtained from the STD evolution of the susceptibility ($\gamma/\nu z$), autocorrelation ($d/z-\theta$) and initial increase of the magnetization (θ). The calculated exponents z, γ/ν and β/ν and the corresponding RG predictions are also included.

L	$\gamma/\nu z$	$d/z-\theta$	θ	z	γ/ν	β/ν
1×10^4	0.87(2)	0.99(1)	0.200(5)	0.840(8)	0.73(2)	0.13(1)
2×10^4	0.88(1)	0.99(1)	0.201(4)	0.839(8)	0.74(1)	0.130(9)
RG			0.2171	0.775	0.75	0.125

In contrast with these measurements, performed by setting $M_0 \equiv 0$, the initial increase of the magnetization has to be measured for vanishingly small values of M_0, as is shown in the figures 8(a) and (b) for system sizes $L = 10^4$ and 2×10^4, respectively. Note that the simulation time verifies that $t \ll t_x$. The insets show the power-law exponents obtained by the fit by means of equation (10) and the extrapolation for $M_0 \to 0$. This procedure yields the θ values reported in table 2 (fourth column) which are close to the RG prediction [1]. Now, by using the relationship $\lambda = d/z - \theta$ and replacing the

J. Stat. Mech. (2011) P09007

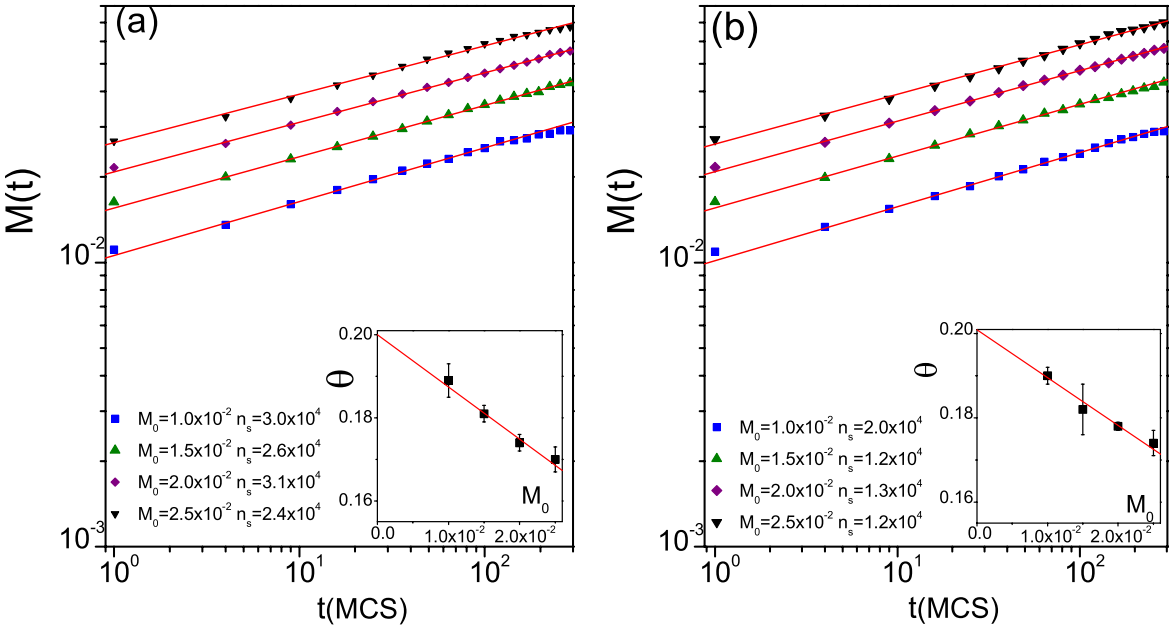

Figure 8. Log–log plot of $M(t)$ versus time showing the initial increase of the magnetization obtained after quenching the system from uncorrelated (disordered) states, with a small magnetization M_0, to T_c. The data correspond to system sizes (a) $L = 10^4$ and (b) $L = 2 \times 10^4$. The solid lines show the fits obtained according to equation (10). The inset shows the linear extrapolation of the values of the exponent to $M_0 \to 0$. The number of averaged configurations (n_s) is also indicated.

exponents determined, one gets the dynamic exponent z (see table 2, fifth column). The value obtained, $z = 0.84$, is consistent with our previous SRD determinations but slightly higher than the RG result ($z_{RG} = 0.775$) [1]. Also, it interpolates between previously published STD results corresponding to a system of size $L = 3000$, which are given by $z = 0.81(1)$ and $0.96(4)$, for $\sigma = 0.70$ and 0.80, respectively [7]. On the other hand, one can use the values of both $\gamma/\nu z$ and z in order to estimate γ/ν (see table 2, sixth column). Furthermore, by assuming that the hyperscaling relationship ($d - 2\beta/\nu = \gamma/\nu$) holds, one can obtain the STD estimation of $\beta/\nu = 0.130(9)$. It is worth mentioning that RG calculations obtained from the asymptotic expansion in $\epsilon = 2\sigma - d$ up to second order yield $\eta = 2 - \sigma = 1.25$ [4]. Then, by using the standard scaling relationships $\gamma/\nu = 2 - \eta$ and $\beta/\nu = (d - 2 + \eta)/2$, the exponents $\gamma/\nu = \sigma = 0.75$ and $\beta/\nu = (d - \sigma)/2 = 0.125$ can be obtained in excellent agreement with our STD estimations.

Furthermore, just by starting with random configurations and measuring the autocorrelation function of the magnetization ($Q(t)$) given by equation (9), one can also obtain the initial increase exponent $\theta = 0.180(6)$, as shown in figure (9). Due to the fact that in this case the fluctuations are more pronounced, the calculation of the correlation function requires better statistics and consequently the simulations were done up to 200 MCS for $L = 10^4$. The error bars include the figures obtained for t_{mic} within the range 4–36 MCS. The value of the exponent θ is close to a previous measurement obtained by using the numerical extrapolation $M_0 \to 0$, namely, $\theta = 0.201(4)$. Furthermore, by using

J. Stat. Mech. (2011) P09007

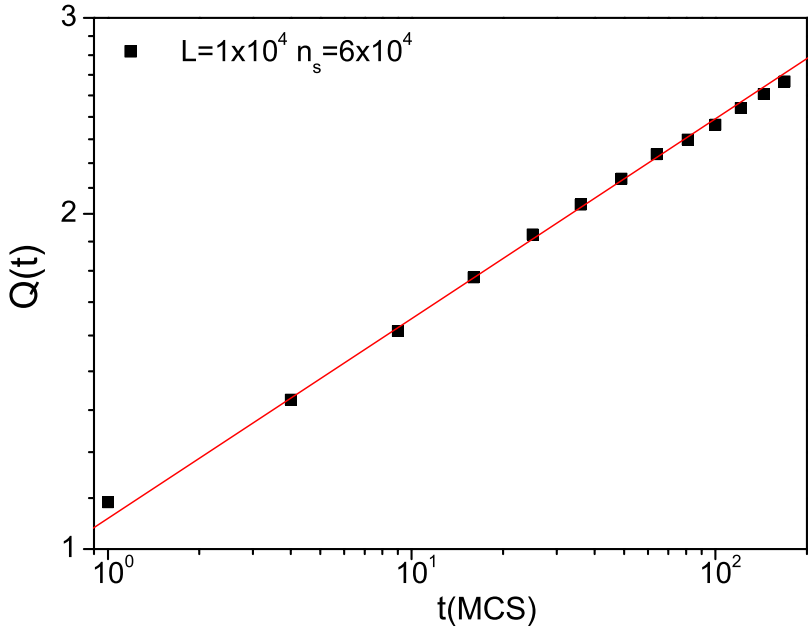

Figure 9. Log–log plot of the time evolution of the autocorrelation function of the magnetization after quenching randomly generated configurations to $T_c = 2.645$. The solid line shows the fit performed with the aid of equation (9). The number of averaged configurations (n_s) and system size (L) are also indicated.

this independent estimation of θ and applying the previously described procedure, the exponents $z = 0.855(9)$, $\gamma/\nu = 0.74(2)$, and $\beta/\nu = 0.13(1)$ can be obtained, which, of course, are in good agreement with our previous estimations.

On the other hand, in order to obtain an additional independent estimation of the dynamic exponent z, the scaling behaviour of the spin–spin correlation functions ($C(t, r)$) was studied for different values of r ranging from 10 to 90 (see the insets of figure 10). The main panels of figure 10 show the best collapse of the $C(r, t)$ obtained by using the conventional critical scaling (equation (5)) and assuming that the hyperscaling relation $d = 2\beta/\nu + \gamma/\nu$ and $\eta = 2 - \gamma/\nu$ hold. From these results, the exponents $z = 0.84(2)$ and $\beta/\nu = 0.125(3)$ were obtained. The error bars were determined by considering the values where noticeable deviations from the collapsed form were observed (not shown here for the sake of space). These results are in excellent agreement with our previous determinations and further support the self-consistency of the results obtained by means of different dynamical methods.

5. Conclusions

In this paper we present and discuss the results of extensive simulations of the nonequilibrium dynamic behaviour of the LR Ising magnet with interactions decaying as $r^{-(d+\sigma)}$, in $d = 1$ dimension and with $\sigma = 0.75$.

Power-law behaviour of the relevant observables was found at temperatures which depend on the interaction range, for both the relaxation and the short-time regimes. The results allow us to verify that the finite-size effect only affects the effective critical

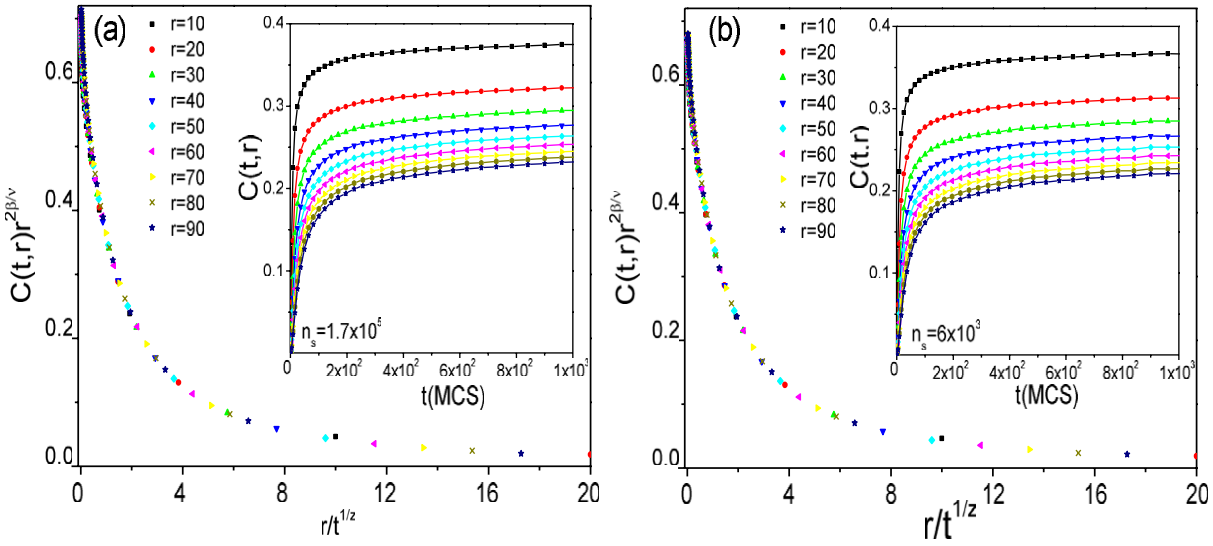

Figure 10. Plots of the scaled spin–spin correlation function $r^{2\beta\nu}C(r,t)$ as a function of the scaled variable $x = r/t^{1/z}$, as obtained for (a) $L = 10^4$ and (b) $L = 2 \times 10^4$. The insets show the time evolution of $C(t,r)$ for the r values indicated, after quenching randomly generated configurations to T_c. The collapses shown in the main panels were obtained by using $z = 0.84$ and $\beta/\nu = 0.125$. The numbers of averaged configurations (n_s) are also indicated.

temperature and the time power-law range, while in contrast the critical exponents remained unaltered within the interaction ranges of the study.

Furthermore, finite-range scaling analysis was applied in order to obtain the critical temperature in the thermodynamic limit which yields $T_c(\infty) = 2.669(1)$. It is found that all the estimated static critical exponents (γ/ν, β/ν, and $1/\nu$) are in good agreement with RG results. Also, the dynamic exponent of the STD initial increase of the magnetization (θ) is close to the RG results. The estimations of the dynamic exponent (z) of the time correlation length from SRD and STD measurements are in agreement, but they are slightly different from the RG results. This difference could be due to insufficiency of the two-loop expansion in the RG analysis, or it may be a consequence of a dependence on the specific Monte Carlo dynamics used (Metropolis in the present paper).

Summing up, the results reported lead us to conclude that the comparison between the two kinds of dynamic measurements, annealing and quenching, provides relevant information on the critical behaviour of a system with long-range interactions, allowing the evaluation of both dynamic and static critical exponents.

Acknowledgments

This work was supported financially by CONICET, UNLP, and ANPCyT (Argentina).

References

[1] Chen Y, Guo S H, Li Z B, Marculescu S and Schuelke L, 2000 *Eur. Phys. J.* B **18** 289
[2] Bergersen B and Rácz Z, 1991 *Phys. Rev. Lett.* **67** 3047
[3] Luijten E and Blote H W J, 1997 *Phys. Rev.* B **56** 8945

J. Stat. Mech. (2011) P09007

[4] Fisher M E, Ma S K and Nickel B G, 1972 *Phys. Rev. Lett.* **29** 8945
[5] Zheng B, 1998 *Int. J. Mod. Phys.* B **12** 1419
[6] Tomé T and de Oliveira M J, 1998 *Phys. Rev.* E **58** 4242
[7] Uzelac K, Glumac Z and Barišć O S, 2008 *Eur. Phys. J.* B **63** 101
[8] Albano E V, Bab M A, Baglietto G, Borzi R A, Grigera T S, Loscar E S, Rodriguez D E, Rubio Puzzo M L and Saracco G P, 2011 *Rep. Prog. Phys.* **74** 026501
[9] Janssen H K, Schaub B and Schmittmann B, 1989 *Z. Phys.* B **73** 539
[10] Santos M and Figueiredo W, 2000 *Phys. Rev.* E **62** 1799
[11] da Silva R, Alves N A and Drugowich de Felício J R, 2002 *Phys. Rev.* E **66** 026130
[12] Bab M A, Fabricius G and Albano E V, 2006 *Phys. Rev.* E **74** 041123
[13] Bab M A, Fabricius G and Albano E V, 2008 *Europhys. Lett.* **81** 10003
[14] Grandi B C S and Figueiredo W, 2004 *Phys. Rev.* E **70** 056109
[15] Chen Y, 2002 *Phys. Rev.* E **66** 037104
[16] Chen Y, Guo S, Li Z and Ye A, 2000 *Eur. Phys. J.* B **15** 97
[17] Baumann F, Dutta S B and Henkel M, 2007 *J. Phys. A: Math. Theor.* **40** 7389
[18] Tomita Y, 2009 *J. Phys. Soc. Japan* **78** 014002
[19] Baglietto G and Albano E V, 2008 *Phys. Rev.* E **78** 021125
[20] Binder K and Luijten E, 2001 *Phys. Rep.* **344** 179
[21] Glumac A and Uzelac K, 1989 *J. Phys. A: Math. Gen.* **22** 4439
[22] Nagle J F and Bonner J C, 1970 *J. Phys. C: Solid State Phys.* **3** 352
[23] Monroe J L, Lucente R and Hourlland J P, 1990 *J. Phys. A: Math. Gen.* **23** 2555
[24] Uzelac K and Glumac Z, 1988 *J. Phys. A: Math. Gen.* **21** L421
[25] Cardy J L, 1984 *J. Phys. A: Math. Gen.* **17** L385
[26] Hohenberg P C and Halperin B I, 1977 *Rev. Mod. Phys.* **49** 435
[27] Humayun K and Bray A J, 1991 *J. Phys. A: Math. Gen.* **24** 1915
[28] Binder K, 1987 *Ferroelectric* **73** 43
[29] Albano E V, Binder K, Heermann D W and Paul W, 1989 *Z. Phys.* B **77** 445
[30] Newman M E J and Barkema G T, 2001 *Monte Carlo Methods in Statistical Physics* (Oxford: Clarendon)
[31] Barati M and Ramazani A, 2000 *Phys. Rev.* B **62** 12130
[32] Okano K, Schülke L, Yamagishi K and Zheng B, 1997 *Nucl. Phys.* B **485** 727
[33] Halperin B I, Hohenberg P C and Ma S-K, 1972 *Phys. Rev. Lett.* **29** 1548

J. Stat. Mech. (2011) P09007